



## OPEN ACCESS

## EDITED BY

Fulvia Palesi,  
University of Pavia, Italy

## REVIEWED BY

Yongxia Zhou,  
University of Southern California,  
United States  
Elena Monai,  
University of Wisconsin-Madison,  
United States

## \*CORRESPONDENCE

Junqiang Lei  
✉ leijq1990@163.com

RECEIVED 20 June 2024

ACCEPTED 19 August 2024

PUBLISHED 29 August 2024

## CITATION

Wang S, Chen X, Zhang Y, Gao Y, Gou L and Lei J (2024) Characterization of cortical volume and whole-brain functional connectivity in Parkinson's disease patients: a MRI study combined with physiological aging brain changes.  
*Front. Neurosci.* 18:1451948.  
doi: 10.3389/fnins.2024.1451948

## COPYRIGHT

© 2024 Wang, Chen, Zhang, Gao, Gou and Lei. This is an open-access article distributed under the terms of the [Creative Commons Attribution License \(CC BY\)](https://creativecommons.org/licenses/by/4.0/). The use, distribution or reproduction in other forums is permitted, provided the original author(s) and the copyright owner(s) are credited and that the original publication in this journal is cited, in accordance with accepted academic practice. No use, distribution or reproduction is permitted which does not comply with these terms.

# Characterization of cortical volume and whole-brain functional connectivity in Parkinson's disease patients: a MRI study combined with physiological aging brain changes

Shuaiwen Wang<sup>1,2,3,4</sup>, Xiaoli Chen<sup>1,2,3,4</sup>, Yanli Zhang<sup>1,2,3,4</sup>, Yulin Gao<sup>1,2,3,4</sup>, Lubin Gou<sup>1,2,3,4</sup> and Junqiang Lei<sup>1,2,3,4\*</sup>

<sup>1</sup>Department of Radiology, The First Hospital of Lanzhou University, Lanzhou, China, <sup>2</sup>Intelligent Imaging Medical Engineering Research Center of Gansu Province, Lanzhou, China, <sup>3</sup>Accurate Image Collaborative Innovation International Science and Technology Cooperation Base of Gansu Province, Lanzhou, China, <sup>4</sup>Gansu Province Clinical Research Center for Radiology Imaging, Lanzhou, China

This study employed multiple MRI features to comprehensively evaluate the abnormalities in morphology, and functionality associated with Parkinson's disease (PD) and distinguish them from normal physiological changes. For investigation purposes, three groups: 32 patients with PD, 42 age-matched healthy controls (HCg1), and 33 young and middle-aged controls (HCg2) were designed. The aim of the current study was to differentiate pathological cortical changes in PD from age-related physiological cortical volume changes. Integrating these findings with functional MRI changes to characterize the effects of PD on whole-brain networks. Cortical volumes in the bilateral temporal lobe, frontal lobe, and cerebellum were significantly reduced in HCg1 compared to HCg2. Although no significant differences in cortical volume were observed between PD patients and HCg1, the PD group exhibited pronounced abnormalities with significantly lower mean connectivity values compared to HCg1. Conversely, physiological functional changes in HCg1 showed markedly higher mean connectivity values than in HCg2. By integrating morphological and functional assessments, as well as network characterization of physiological aging, this study further delineates the distinct characteristics of pathological changes in PD.

## KEYWORDS

fMRI, Parkinson's disease, cortex, morphology, functional connectivity

## Introduction

Parkinson's disease (PD) manifests with a diverse range of symptoms, primarily sensory-motor in nature. As the disease progresses, patients often develop a spectrum of non-motor symptoms that complicate the clinical picture. Neuropathological studies have consistently highlighted characteristic degenerative changes in the substantia nigra (SN)-striatal pathway in individuals diagnosed with PD (Furukawa et al., 2022; Pineda-Pardo et al., 2022). With advances in MRI technology, changes in the substantia nigra, such as the loss of the swallow-tail

sign, are observed in susceptibility-weighted imaging (SWI) and can occur in neurodegenerative disorders such as PD, dementia with Lewy bodies (DLB) (Prasuhn et al., 2021; Tseriotis et al., 2024). Additionally, novel research methods have played an important role in studying the morphology and functional brain activity of the whole brain in PD.

In studies of brain morphology, it is well-documented that both gray and white matter atrophy are commonly observed in healthy older adults (Thambisetty et al., 2010). Numerous researchers have demonstrated that cortical volume changes due to aging are a physiological process. Understanding the distribution and timing of these morphological changes during normal aging is crucial for distinguishing between physiological and pathological alterations. Imaging studies have shown that brain volume, indicated by pixel dimensions in T1 anatomical MRI images, is significantly correlated with age-related changes in specific regions such as the dorsal prefrontal lobe, the internal olfactory cortex, and the temporal lobe (Thomann et al., 2013; Wang et al., 2019; Christova and Georgopoulos, 2023). However, studies analyzing the relationship between cortical volume and task-regulatory function have found that performance on certain tasks is not affected by normal physiological volume changes (Shaked et al., 2018). In contrast to the effects of aging on brain volume, studies of brain volume changes in people with PD have shown different volume changes in the anterior and posterior lobes of the cerebellum, areas associated with higher-level functions such as complex movement, task design, and learning (Wagner et al., 2021; van Dun et al., 2022; Kerestes et al., 2023). Some studies report no significant differences in overall brain volume between patients with the “brain-first” subtype of PD (where initial  $\alpha$ -synuclein pathology arises inside the central nervous system) and healthy controls (Banwinkler et al., 2022). Similar findings have been reported in PD patients without cognitive impairments when compared to age-matched controls (Tessitore et al., 2012). Evidently, the theories of aging and PD brain volume changes are still at a controversial stage. Although these studies illuminate some physiological and pathological changes, the study of characteristic brain functional network changes corresponding to different morphologies might better reflect the functional characteristics represented by brain volume at different stages. This approach could enhance our understanding of the various cortical volume changes observed in patients with PD.

Functional MRI (fMRI) is a powerful tool for assessing the functional activities and interconnections between different brain regions, providing a quantitative approach for brain network research. Some studies have noted an increase in spontaneous brain region activity (ALFF) in older adults, although the connectivity between functional language networks appears to decrease (Zhang et al., 2021). As individuals age, advanced cognitive networks such as the default mode and executive control networks tend to shift from a decentralized to a more localized topology (Li et al., 2013). In contrast, the structure of primary sensory and motor networks remains relatively stable with age compared to higher cognitive networks (Thambisetty et al., 2010). Graph theory analyses by Wang et al. suggest that brain integration decreases with age, though clustering coefficients increase, preserving a stable small-world property (Alloza et al., 2018). This highlights the brain's robustness, maintaining dynamic equilibrium through compensatory mechanisms despite regional functional declines due to aging. In PD, studies on brain functional network have not only focused on motor function symptoms but also revealed abnormalities in the brainstem-thalamus and striatal-cortical connectivity (Bostan and Strick, 2018; Johansson et al., 2022; Pimentel et al., 2023). And in

PD patients with abnormal swallowtail sign, Zhou found that the substantia nigra, red nucleus, hypothalamus, thalamus, ventral striatum, caudate, lingual gyrus, postcentral gyrus, frontal pole and temporal cortex had reduced functional connectivity with voxel-mirrored homotopic correlation (VMHC) (Zhou, 2021). Additionally, enhanced functional connectivity (FC) between the cerebellum and sensorimotor network was observed in PD patients (Tolosa et al., 2021). Hyperconnectivity in motor, supplementary motor, dorsolateral prefrontal, and visual cortex has been suggested, with global efficiencies based on functional connectivity being lower in PD patients, while local efficiencies are slightly higher, potentially due to compensatory effects (Zhou, 2021). Research on non-motor symptoms has indicated significant correlations between the severity of these symptoms in PD patients and altered FC in the ipsilateral prefrontal and anterior cingulate cortex (Jellinger, 2015). Cognitive function impairments and connectivity changes in the cerebellum-sensorimotor network-dorsal attentional network have been noted as well. In PD patients with mild cognitive impairment (MCI), FC was notably reduced between the default mode network (DMN) and regions such as the middle frontal gyrus and middle temporal gyrus. Within the DMN, connections between the anterior temporal lobe and inferior frontal gyrus were also diminished (Hou et al., 2016). Further, the posterior cingulate cortex showed reduced connectivity with various regions in PD-MCI patients compared to those without cognitive impairment (Carey et al., 2021). Gorges et al. (2015) suggested that increased FC in PD patients without cognitive impairment might act as a compensatory mechanism prior to the onset of PD-MCI.

Despite the insightful findings mentioned above, they do not fully differentiate between age-related physiological intracerebral changes and those specific to PD. Consequently, this study was designed to assess and characterize cortical volume changes using voxel-based morphometric analysis (VBM). VBM is a neuroimaging technique for studying focal differences in brain anatomy, reflecting anatomical differences by quantifying the density or volume of gray and white matter for each voxel in MRI scans. To further enhance our understanding, we integrated the analysis of whole brain functional network connection using the Network-based statistic (NBS) method. It provides a comprehensive analysis of brain network integrity. Unlike methods focusing on individual region connections, NBS examines the entire brain network to identify abnormal connectivity, reflecting both physiological and pathological statuses, and has been widely utilized in studies of PD, AD, schizophrenia, and other neurological conditions (Zhan et al., 2019). By employing these approaches, we aim to comprehensively assess the pathological brain morphological features associated with physiological aging and PD, as well as the differences in whole-brain network connectivity that these features reflect.

## Methods

### Subjects

This prospective study was approved by the Ethics Committee of the First Hospital of Lanzhou University. A total of 40 patients diagnosed with PD and 83 healthy controls were recruited for the study. The controls were divided into two groups: 50 individuals aged 50–85 years, matched in age with the PD patients (HCg1), and 33 young and middle-aged adults aged 20–40 years (HCg2). PD diagnoses

were confirmed by two experienced neurologists at the First Hospital of Lanzhou University, adhering to the diagnostic criteria established by the UK Parkinson's Disease Society Brain Bank.

Exclusion criteria for participation included: (1) a history of head surgery, trauma, or neurotoxic drug use; (2) claustrophobia, depression, dementia, or history of psychotropic drug use; (3) other neurological or psychiatric disorders; (4) substantial deformation of brain structure due to cerebral infarction, hemorrhage, or atrophy that could interfere with MRI analysis; (5) excessive head movement during scanning, defined as greater than 2.5 mm movement or a rotation angle exceeding 2.5° during post-processing; (6) presence of dentures or other metallic head and facial implants. Patients with PD additionally need to be excluded those with pyramidal, cerebellar dysfunction, gaze paresis and autonomic dysfunction in neurologic examination, visual or hearing impairments, and those receiving device-assisted therapies (e.g., DBS). Ultimately, 32 PD patients and 75 healthy controls (42 in HCg1, 50–80 years old, and 33 in HCg2: 20–40 years old) were included in the study. All PD patients were assessed using the Unified Parkinson's Disease Rating Scale, Part III (UPDRS-III), to evaluate dyskinesia and were required not to take any anti-Parkinson medication for 12 h before MRI scanning. Cognitive function was assessed using the Mini-Mental State Examination (MMSE), and handedness was evaluated with the Edinburgh Handedness Inventory. Demographic data, including age and educational background, were recorded for all participants. Each subject provided informed consent prior to their inclusion in the study.

## Image scanning

Data acquisition was conducted on a Siemens MAGNETOM Skyra 3.0 Tesla MRI scanner. The parameters setting T1-weighted structural images were acquired using the MPRAGE sequence, with parameters: TE = 2.32 ms, TR = 2,300 ms, flip angle = 8°, a 256 × 256 matrix, a slice thickness of 0.9 mm, and 192 slicers. Functional brain studies and network analyses employed BOLD sequences with echo planar imaging scans, which included settings of TE = 30 ms, TR = 3,200 ms, flip angle = 90°, matrix = 64 × 64, slice thickness = 3 mm, number of slices = 40, and 200 time points.

## Demographic and clinical data analysis

The demographic and clinical data for both the PD and HCg1 groups, HCg1 and HCg2 were analyzed using SPSS software (version 26). Categorical variables such as gender and habitual hand use were assessed using the Chi-square ( $\chi^2$ ) test, while continuous variables, including age and years of education, were analyzed using the two-sample t-test. Statistical significance was determined at a threshold of  $p < 0.01$ .

## Cerebral cortex volume analysis

The T1 structural images were processed using the DPABI 6.2v toolkit<sup>1</sup> and SPM 12<sup>2</sup> on the MATLAB 2021b platform. The images

were normalized to the Montreal Neurological Institute (MNI) space in Montreal, Canada, and segmented into cortical, white matter, and cerebrospinal fluid components. For data smoothing, a full-width-at-half-maximum (FWHM) Gaussian kernel of 8 mm was applied, and the voxels were resampled to a 3 mm size. VBM was employed to assess tissue volume by quantifying the image voxels. Statistical analysis involved the use of independent samples t-tests to compare differences in cerebral cortical volume among the groups, specifically between PD and HCg1, HCg1 and HCg2. Significance levels were set at  $p < 0.05$ , with multiple comparison corrections applied using the false discovery rate (FDR) at  $p < 0.01$ . Age and years of education were included as covariates in the analysis between PD and HCg1, and years of education was included as covariates in the analysis between HCg1 and HCg2 to account for its potential influence on the results.

## Analysis of whole brain functional connection

Brain structural and functional MRI images were preprocessed and analyzed using the Brain Functional Connectivity Toolkit CONN 22a<sup>3</sup> on the MATLAB 2021b platform. The preprocessing workflow in the CONN pipeline included steps such as head motion correction, unwarping, slice-timing correction, segmentation and realignment, and normalization to the MNI space. Data smoothing was achieved with an 8 mm Gaussian filter, and physiological noise was reduced using aCompCor to enhance functional connectivity results. Scans affected by excessive head motion were flagged and excluded using the artifact rejection toolbox, set at the 97th percentile.<sup>4</sup> BOLD signals that deviated from the global mean by  $\pm 5$  standard deviations or showed intra-frame shifts of at least 0.9 mm were considered artifacts and removed during the denoising process. In the comparison of HCg1 and HCg2, covariates in the analysis included default CONN settings, and years of education. In the comparison of PD with HCg2, covariates were added to age, in addition to the previously listed parameters. Temporal band-pass filtering was applied to isolate low-frequency fluctuations within the 0.008 to 0.09 Hz range, thereby enhancing the signal-to-noise ratio. Connectivity analysis was conducted using region-to-region connectivity (RRC) across all brain regions for comparisons between PD and HCg1, and between HCg1 and HCg2 within each brain functional network. Network-based statistics (NBS), a nonparametric, cluster-level statistical technique using graph-theoretic concepts, was employed to address multiple comparison (Zalesky et al., 2010, 2012). NBS facilitates the rejection of the null hypothesis at the network level, allowing the detection of significant network clusters rather than individual connections. In the application of NBS to examine group differences, an initial uncorrected  $p$ -value threshold of  $< 0.001$  was used for each contrast in connection strengths. Mean values of overall network connectivity were assessed with a threshold of  $p < 0.05$  and corrected for FDR at  $< 0.01$ . In this study, we analyzed whole brain networks and brain regions, including DMN, Sensorimotor Network (SMN), Visual Network (VN), Salience Network (SN), Dorsal Attention Network (DAN), Frontal Parietal Network (FPN), Language Network (LN),

1 <http://rfmri.org/dpabi>

2 <https://www.fil.ion.ucl.ac.uk/spm/software/download>

3 <https://www.nitrc.org/projects/conn>

4 [https://www.nitrc.org/projects/artifact\\_detect](https://www.nitrc.org/projects/artifact_detect)

Dorsal Parietal Network (DPN) and the 132 brain regions and subregions (see [Supplementary Table](#)).

## Results

### Results of demographic and clinical data analysis

Statistical analysis revealed significant differences in years of education and MMSE scores between the age matched control group (HCg1) and the young and middle-aged control group (HCg2), with  $p$ -values less than 0.01. There was also a significant age difference between the PD group and HCg1 ( $p < 0.01$ ). However, no significant difference in MMSE scores was observed between these two groups (see [Table 1](#)).

### Analysis results for cerebral cortical volume

VBM analysis demonstrated that there were changes in cortical volumes between HCg1 and HCg2, notably in the bilateral cerebellum (including the anterior and posterior lobes and cerebellar regions 4 and 5, and right region 6), bilateral temporal lobes (including the middle and inferior temporal gyrus), and the medial prefrontal lobes (comprising the cingulate gyrus, superior frontal gyrus, middle frontal gyrus, inferior frontal gyrus, and parts of the motor cortex). There was also a significant reduction in the cortical volume of the bilateral insula. However, no significant changes in cortical volume were found between the PD group and HCg1 (see [Table 2](#) and [Figure 1](#)).

### Results of functional connectivity analysis

In our RRC functional connectivity analysis, we observed that individuals with PD demonstrated reduced functional connectivity between the DMN, Precuneus, and various regions, including the bilateral motor cortex, parietal lobe (specifically the inferior parietal lobe within the dorsal attentional network), bilateral temporal lobe, cerebellum and frontal lobe ( $p < 0.001$  uncorrected). Additionally, connectivity between the temporal and frontal lobes was notably decreased in the PD group compared to the control group (HCg1) ( $p < 0.001$  uncorrected). Whereas elevated functional connectivity was seen between the parietal portion of the DMN and the bilateral

temporal lobes, as well as with the left frontal pole ( $p < 0.001$  uncorrected). In comparisons showing differential functional connectivity effect, the PD group showed reduced mean functional connectivity across the brain, which was statistically significant ( $p < 0.05$ , FDR  $< 0.01$ ) (see [Figure 2](#) and [Table 3](#)). Comparative analysis between the age matched control group (HCg1) and the young and middle-aged control group (HCg2) revealed enhanced functional connectivity in several regions. These included between the sensorimotor cortex and the left frontal lobe (including the ACC of the attentional network), between the left putamen/accumbens and the right frontal and temporal lobes, and between the visual cortex (calcarine cortex, cuneus) and the supramarginal gyrus ( $p < 0.001$  uncorrected). Further, there was enhanced connectivity linking the hippocampus with the motor cortex, the attentional network with the basal ganglia, the basal ganglia with the cerebellum, the cerebellum with the paracingulate gyrus, and the subcallosal gyrus with the superior frontal gyrus ( $p < 0.001$  uncorrected). Overall, the mean functional connectivity of the entire brain network was significantly higher in HCg1 compared to HCg2 ( $p < 0.05$ , FDR  $< 0.01$ ) (see [Figure 2](#) and [Table 3](#)).

## Discussion

In our study, we conducted a comprehensive analysis of changes in cortical volume, and brain network function due to both aging and PD. It is well-established that changes in brain volume are a physiological phenomenon throughout the aging process. This physiological state involves a complex interplay of multiple mechanisms, including protein conversion, mitochondrial metabolism, neuroinflammation, and oxidative stress, all of which contribute to the aging process ([Wagner et al., 2016](#); [Vecchio et al., 2022](#)). When comparing the age matched control group (HCg1) with the young and middle-aged control group (HCg2), significant reductions in cortical volume were observed in HCg1 across multiple regions, including the bilateral cerebellum, temporal lobes, frontal lobes, and insula. Previous research has identified that atrophy in older adults is most pronounced in the medial prefrontal cortex (PFC), followed by the dorsolateral prefrontal cortex, temporal and parietal cortical areas, hippocampus, and caudate nucleus, which aligning with our findings ([Dennis et al., 2007](#); [Fjell and Walhovd, 2010](#)). However, unlike neurodegenerative conditions such as AD and PD, such extensive volumetric atrophy in healthy aging has not been linked to significant cognitive and sensorimotor impairments. This

TABLE 1 Demographic data of the prospective study group.

	PD ( $n = 32$ )	HCg1 ( $n = 42$ )	HCg2 ( $n = 33$ )	$P_{PD \text{ vs. HCg1}}$	$P_{HCg1 \text{ vs. HCg2}}$
Age (years)	69.531 $\pm$ 9.287	62.262 $\pm$ 8.923	32.939 $\pm$ 5.069	0.001*	0.000*
Gender (M/F)	19/13	23/19	20/13	0.691	0.617
Education (years)	10.625 $\pm$ 3.160	10.952 $\pm$ 3.854	15.454 $\pm$ 1.519	0.701	0.000*
Dominant hand (left/right)	2/30	0/42	1/32	0.133	0.256
Disease duration (years)	5.219 $\pm$ 2.484	–	–	–	–
UPDRS-III score	23.219 $\pm$ 5.549	–	–	–	–
MMSE	27.063 $\pm$ 1.368	27.476 $\pm$ 1.200	28.182 $\pm$ 0.869	0.177	0.006*

Data are represented as Mean  $\pm$  SD.

PD, Parkinson's Disease; HC, Healthy Control; MMSE, Mini Mental State Exam; UPDRS-III, Unified Parkinson's Disease Rating Scale Part III. \* $p$  value  $< 0.01$ .

TABLE 2 Analysis of cortical volume of HCg1 vs. HCg2 brains.

Brain regions		Cluster size	Coordinate	Peak value
Right cerebellum	Cerebellum anterior lobe	631	30, -45, -42	-6.659
	Cerebellum posterior lobe	456		
	Cerebellum_Crus1	272		
	Cerebellum_4_5	166		
	Cerebellum_6	127		
Left cerebellum	Cerebellum posterior lobe	259	-30, -42, -42	-6.451
	Cerebellum_Crus1	232		
	Cerebellum_4_5	174		
Left temporal lobe	Temporal_Mid	359	-63, -18, -18	-5.273
	Temporal_Inf	174		
Right temporal lobe	Temporal_Mid	311	51, -21, -27	-4.788
	Temporal_Inf	250		
Medial prefrontal lobe	Cingulum_Ant_L	151	3, 33, 30	-5.478
	Cingulum_Ant_R	62		
	Cingulum_Mid_L	141		
	Cingulum_Mid_R	136		
	Frontal_Sup_Medial_L	109		
	Frontal_Sup_R	91		
	Frontal_Sup_Orb_L	52		
	Supp_Motor_Area_L	48		
Right frontal lobe	Frontal_Inf_Oper	147	42, 9, 33	-6.761
	Frontal_Inf_Tri	128		
	Frontal_Mid	95		
	Precentral	65		
	Rolandic_Oper	65		
Right insula	Insula	68	-54, 9, 0	-5.210
Left insula	Insula	141		

L, Left; R, Right; Mid, Middle; Inf, inferior; Ant, Anterior; Sup, Superior; Orb, Orbital; Frontal\_Inf\_Oper, Frontal inferior opercular; Tri, Triangular; Rolandic Oper, Rolandic operculum.

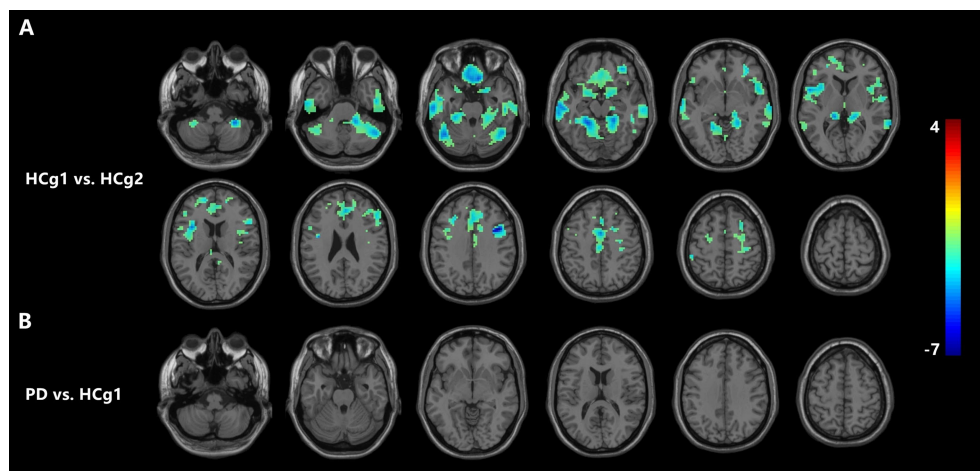
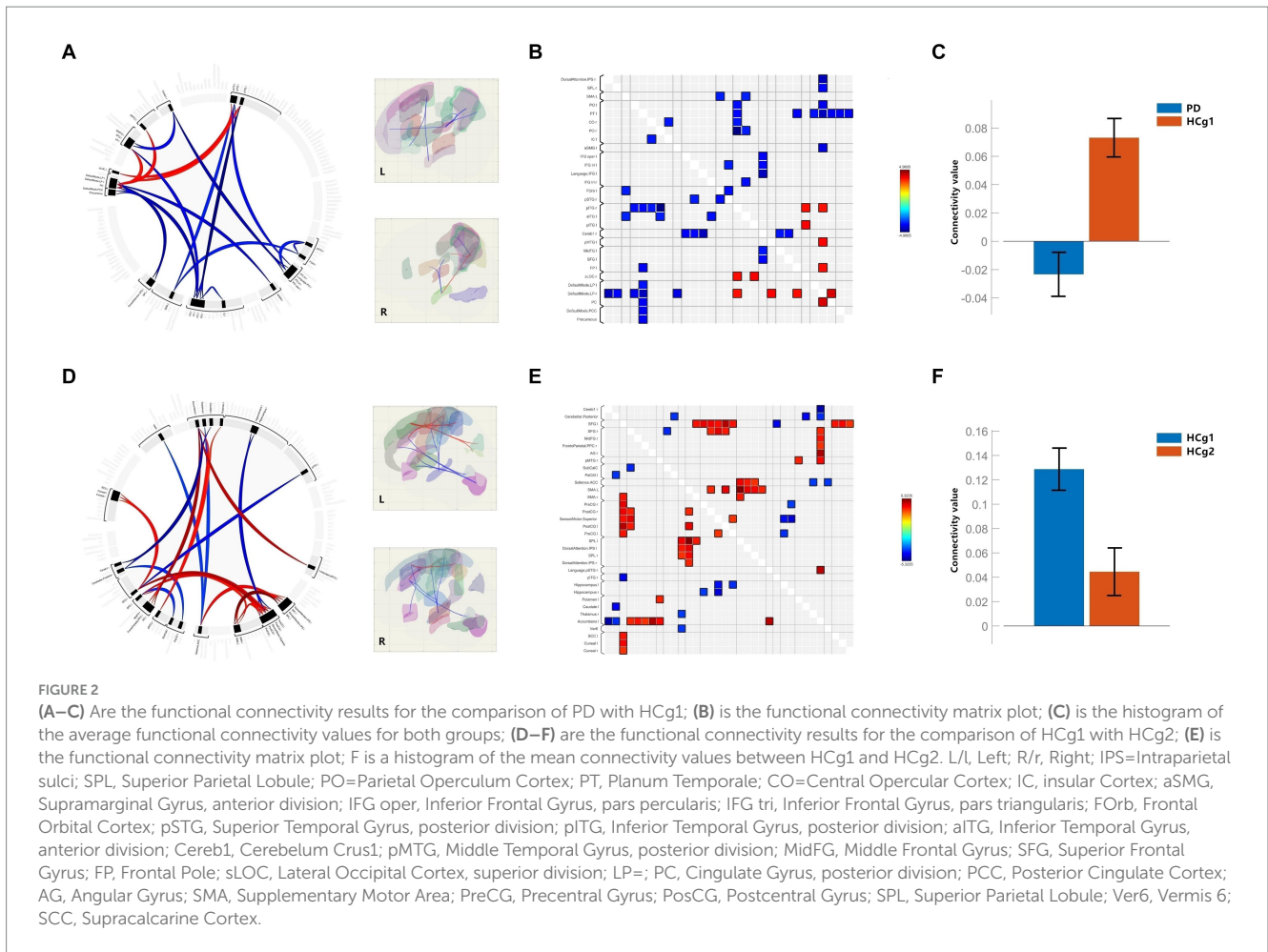


FIGURE 1 (A) Illustrates a significant reduction in cortical volume in HCg1 compared to HCg2 (blue area). The areas of difference include the bilateral cerebellum, frontal lobe, temporal lobe, and insula ( $p < 0.05$ , FDR correction  $p < 0.01$ ). As shown in (B), there was no significant change in the cortical volume of the PD group compared to the HCg1 group.



**TABLE 3** Comparative analysis of PD vs. HCg1 and HCg1 vs. HCg2 whole-brain network connectivity.

	T value	p uncorrected	p-FDR
Network <sub>PD vs. HCg1</sub>	-7.79	0.000	0.000
Network <sub>HCg1 vs. HCg2</sub>	5.37	0.000	0.000

suggests that physiological brain atrophy is accompanied by a dynamic equilibrium in the overall brain network, likely due to compensatory mechanisms. The network properties of the aging brain, specifically its small-world characteristics, have been the focus of several studies. These studies found that the average degree and path length differ between younger and older adults; the younger group exhibited lower average path length values, indicating a highly integrated functional network. Conversely, older adults displayed higher clustering coefficients (Goldman et al., 2012; Mancho-Fora et al., 2020), suggesting more localized connectivity. In contrast to normal aging, the brain network in PD patients demonstrates an imbalance in compensatory mechanisms, yet without significant morphological changes initially. Research has suggested that brain volume atrophy observed in later stages of PD is associated with the development of multiple complications (Lewis et al., 2016; Filippi et al., 2020). Therefore, it is critical to explore characteristic changes in brain networks in PD patients before significant volumetric changes occur,

as this can provide valuable insights into the disease’s progression and associated complications.

In our continued exploration of brain function, we have focused on functional connection across various brain networks, including the DMN, SMN, VN, SN, DAN, FPN, LN, DPN and the 132 brain regions and subregions. NBS was utilized to compare the mean connectivity coefficients between groups, particularly highlighting differences between the older control group (HCg1) and the PD group, as well as between HCg1 and the young and middle-aged control group (HCg2). In patients with PD, our analysis revealed significant connectivity differences in networks, including the DMN, DAN, and LN. Functional connectivity abnormalities were predominantly noted between several brain regions within the parietal, temporal, and frontal lobes, which are primarily associated with higher-level sensory, motor, and cognitive control functions. Interestingly, these abnormal connections were not observed among the primary sensorimotor cortex and related networks such as the precentral gyrus, postcentral gyrus, and SMN. Conversely, the comparison between HCg1 and HCg2 revealed increased functional connectivity within the SMN and primary sensorimotor cortex (precentral gyrus, postcentral gyrus) and the supplementary motor area (SMA). Furthermore, the SN, LN, and DAN showed enhanced connectivity with various brain regions. These differences were more pronounced in the anterior regions of the brain, possibly correlating with the distribution of cortical atrophic areas.

Additionally, the overall mean functional connectivity values were significantly higher in HCg1 compared to HCg2, suggesting an age-related compensatory mechanism in network function. Previous research has not only highlighted the prevalence of brain volume atrophy in older individuals but has also underscored the compensatory functions for cognition and language through various aspects such as neuropathology and brain networks (Lighthall et al., 2014; Di Tella et al., 2021). Furthermore, studies have noted a posterior–anterior shift in aging (PASA) that reflects a migration of active brain areas from the occipital to the frontal lobe with advancing age (Davis et al., 2008; Lamar et al., 2014; Rosjat et al., 2021). Our study also identified enhanced functional connectivity in HCg1 among multiple regions in the frontal lobe (Figures 2D–E). In the PD group, we observed negative mean network connectivity values in PD patients compared to the normal population of the same age, demonstrating a significant decline in the physiological mechanisms of brain networks. With reference to the distribution of functional brain connectivity caused by aging, most of the abnormal connectivity areas in PD patients were located in the posterior part of the brain (parietal and occipital lobes) (Figures 2A,B), suggesting a physiological imbalance in the posterior cerebral network following the onset of PD. Research has also indicated that PD patients' brains exhibit more vulnerable small-world properties than their healthy counterparts (Suo et al., 2017; Kok et al., 2020; Zuo et al., 2023), supporting the findings of this study and highlighting the complex interplay of degenerative processes in PD.

## Limitation

A limitation of this study is the relatively small sample size and the lenient criteria for head movement during scans. Plans are underway to address these shortcomings in subsequent studies by including a larger cohort and implementing stricter movement control measures to enhance the reliability and validity of our findings. Additionally, in the analysis of brain volume in PD patients, there is a lack of exploration of cortical morphological changes in patients with later stages of the disease or in the presence of complications such as cognitive impairment. This necessitates expanding the sample size, along with follow-up and multiple MRI scans, to clarify the clinically characteristic changes in patients with PD who exhibit significant brain volume atrophy during the disease course. Combining this with functional network analysis will help us understand the specific changes in PD more clearly and assess disease progression more accurately.

## Conclusion

Through our comprehensive analysis of physiological brain morphological features, and functional networks, we have enhanced our understanding of the distinct MRI characteristics associated with PD. Notably, the volumetric analysis in this study did not reveal significant abnormalities in PD patients, but in the NBS, we observed a significant difference in the mean connectivity values of PD compared to age-matched controls (HCg1). The distribution of these connectivity discrepancy regions also differs from the distribution of

network connectivity anomalies caused by aging. This may be because the cases primarily exhibit sensorimotor dysfunctions without cognitive or non-motor symptoms, resulting in less notable changes in cortical volume. However, more significant differences and distributional features have emerged in brain network functional connectivity. In future research, we aim to incorporate a study group that specifically focuses on the complexities and complications associated with PD. This approach will allow for a more thorough investigation of both morphological and functional changes linked to the disease.

## Data availability statement

The original contributions presented in the study are included in the article/[Supplementary material](#), further inquiries can be directed to the corresponding author.

## Ethics statement

The studies involving humans were approved by the Ethics Committee of the First Hospital of Lanzhou University. The studies were conducted in accordance with the local legislation and institutional requirements. The participants provided their written informed consent to participate in this study. Written informed consent was obtained from the individual(s) for the publication of any potentially identifiable images or data included in this article.

## Author contributions

SW: Data curation, Funding acquisition, Investigation, Methodology, Software, Writing – original draft. XC: Data curation, Formal analysis, Funding acquisition, Investigation, Writing – review & editing. YZ: Data curation, Formal analysis, Methodology, Writing – review & editing. YG: Formal analysis, Resources, Writing – review & editing. LG: Data curation, Formal analysis, Software, Writing – review & editing. JL: Conceptualization, Resources, Supervision, Writing – review & editing.

## Funding

The author(s) declare that financial support was received for the research, authorship, and/or publication of this article. This study was supported by Gansu Provincial Youth Science and Technology Fund Scheme, Grant/Award Number: 21JR11RA071, the funder is Xiaoli Chen, the second author of the manuscript and the First Hospital of Lanzhou University In-Hospital Fund, Grant/Award Number: 2020-41, the funder is Shuaiwen Wang, the first author of the manuscript.

## Acknowledgments

We thank all the authors for their work on this study, and also the patients and their families for their constructive cooperation during the study participation.

## Conflict of interest

The authors declare that the research was conducted in the absence of any commercial or financial relationships that could be construed as a potential conflict of interest.

## Publisher's note

All claims expressed in this article are solely those of the authors and do not necessarily represent those of their affiliated

organizations, or those of the publisher, the editors and the reviewers. Any product that may be evaluated in this article, or claim that may be made by its manufacturer, is not guaranteed or endorsed by the publisher.

## Supplementary material

The Supplementary material for this article can be found online at: <https://www.frontiersin.org/articles/10.3389/fnins.2024.1451948/full#supplementary-material>

## References

- Alloza, C., Cox, S. R., Blesa Cabez, M., Redmond, P., Whalley, H. C., Ritchie, S. J., et al. (2018). Polygenic risk score for schizophrenia and structural brain connectivity in older age: a longitudinal connectome and tractography study. *NeuroImage* 183, 884–896. doi: 10.1016/j.neuroimage.2018.08.075
- Banwinkler, M., Dzialas, V., Hoenig, M. C., and van Eimeren, T. (2022). Gray matter volume loss in proposed brain-first and body-first Parkinson's disease subtypes. *Mov. Disord.* 37, 2066–2074. doi: 10.1002/mds.29172
- Bostan, A. C., and Strick, P. L. (2018). The basal ganglia and the cerebellum: nodes in an integrated network. *Nat. Rev. Neurosci.* 19, 338–350. doi: 10.1038/s41583-018-0002-7
- Carey, G., Görmezoğlu, M., de Jong, J., Hofman, P., Backes, W. H., Dujardin, K., et al. (2021). Neuroimaging of anxiety in Parkinson's disease: a systematic review. *Mov. Disord.* 36, 327–339. doi: 10.1002/mds.28404
- Christova, P., and Georgopoulos, A. P. (2023). Changes of cortical gray matter volume during development: a human connectome project study. *J. Neurophysiol.* 130, 117–122. doi: 10.1152/jn.00164.2023
- Davis, S. W., Dennis, N. A., Daselaar, S. M., Fleck, M. S., and Cabeza, R. (2008). Que PASA? The posterior-anterior shift in aging. *Cereb. Cortex* 18, 1201–1209. doi: 10.1093/cercor/bhm155
- Dennis, N. A., Daselaar, S., and Cabeza, R. (2007). Effects of aging on transient and sustained successful memory encoding activity. *Neurobiol. Aging* 28, 1749–1758. doi: 10.1016/j.neurobiolaging.2006.07.006
- Di Tella, S., Blasi, V., Cabini, M., Bergsland, N., Buccino, G., and Baglio, F. (2021). How do we Motorically resonate in aging? A compensatory role of prefrontal cortex. *Front. Aging Neurosci.* 13:694676. doi: 10.3389/fnagi.2021.694676
- Filippi, M., Sarasso, E., Piramide, N., Stojkovic, T., Stankovic, I., Basaia, S., et al. (2020). Progressive brain atrophy and clinical evolution in Parkinson's disease. *Neuroimage Clin.* 28:102374. doi: 10.1016/j.nicl.2020.102374
- Fjell, A. M., and Walhovd, K. B. (2010). Structural brain changes in aging: courses, causes and cognitive consequences. *Rev. Neurosci.* 21, 187–221. doi: 10.1515/revneuro.2010.21.3.187
- Furukawa, K., Shima, A., Kambe, D., Nishida, A., Wada, I., Sakamaki, H., et al. (2022). Motor progression and nigrostriatal neurodegeneration in Parkinson disease. *Ann. Neurol.* 92, 110–121. doi: 10.1002/ana.26373
- Goldman, J. G., Stebbins, G. T., Bernard, B., Stoub, T. R., Goetz, C. G., and de Toledo-Morrell, L. (2012). Entorhinal cortex atrophy differentiates Parkinson's disease patients with and without dementia. *Mov. Disord.* 27, 727–734. doi: 10.1002/mds.24938
- Gorges, M., Müller, H. P., Lulé, D., Pinkhardt, E. H., Ludolph, A. C., and Kassubek, J. (2015). To rise and to fall: functional connectivity in cognitively normal and cognitively impaired patients with Parkinson's disease. *Neurobiol. Aging* 36, 1727–1735. doi: 10.1016/j.neurobiolaging.2014.12.026
- Hou, Y., Yang, J., Luo, C., Song, W., Ou, R., Liu, W., et al. (2016). Dysfunction of the default mode network in drug-naïve Parkinson's disease with mild cognitive impairments: a resting-state fMRI study. *Front. Aging Neurosci.* 8:247. doi: 10.3389/fnagi.2016.00247
- Jellinger, K. A. (2015). Neuropathobiology of non-motor symptoms in Parkinson disease. *J. Neural. Transm. (Vienna)* 122, 1429–1440. doi: 10.1007/s00702-015-1405-5
- Johansson, M. E., Cameron, I., Van der Kolk, N. M., de Vries, N. M., Klimars, E., Toni, I., et al. (2022). Aerobic exercise alters brain function and structure in Parkinson's disease: a randomized controlled trial. *Ann. Neurol.* 91, 203–216. doi: 10.1002/ana.26291
- Kerestes, R., Laansma, M. A., Owens-Walton, C., Perry, A., van Heese, E. M., Al-Bachari, S., et al. (2023). Cerebellar volume and disease staging in Parkinson's disease: an ENIGMA-PD study. *Mov. Disord.* 38, 2269–2281. doi: 10.1002/mds.29611
- Kok, J. G., Leemans, A., Teune, L. K., Leenders, K. L., McKeown, M. J., Appel-Cresswell, S., et al. (2020). Structural network analysis using diffusion MRI Tractography in Parkinson's disease and correlations with motor impairment. *Front. Neurol.* 11:841. doi: 10.3389/fneur.2020.00841
- Lamar, M., Craig, M., Daly, E. M., Cutter, W. J., Tang, C., Brammer, M., et al. (2014). Acute tryptophan depletion promotes an anterior-to-posterior fMRI activation shift during task switching in older adults. *Hum. Brain Mapp.* 35, 712–722. doi: 10.1002/hbm.22187
- Lewis, M. M., Du, G., Lee, E. Y., Nasrallah, Z., Sterling, N. W., Zhang, L., et al. (2016). The pattern of gray matter atrophy in Parkinson's disease differs in cortical and subcortical regions. *J. Neurol.* 263, 68–75. doi: 10.1007/s00415-015-7929-7
- Li, X., Pu, F., Fan, Y., Niu, H., Li, S., and Li, D. (2013). Age-related changes in brain structural covariance networks. *Front. Hum. Neurosci.* 7:98. doi: 10.3389/fnhum.2013.00098
- Lighthall, N. R., Huettel, S. A., and Cabeza, R. (2014). Functional compensation in the ventromedial prefrontal cortex improves memory-dependent decisions in older adults. *J. Neurosci.* 34, 15648–15657. doi: 10.1523/JNEUROSCI.2888-14.2014
- Mancho-Fora, N., Montalà-Flaquer, M., Farràs-Permanyer, L., Bartrés-Faz, D., Vaque-Alcázar, L., Peró-Cebollero, M., et al. (2020). Resting-state functional dynamic connectivity and healthy aging: a sliding-window network analysis. *Psicothema* 32, 337–345. doi: 10.7334/psicothema2020.92
- Pimentel, J. M., Moiola, R. C., De Araujo, M., and Vargas, P. A. (2023). An integrated Neurorobotics model of the cerebellar-basal ganglia circuitry. *Int. J. Neural Syst.* 33:2350059. doi: 10.1142/S0129065723500594
- Pineda-Pardo, J. A., Sánchez-Ferro, Á., Monje, M., Pavese, N., and Obeso, J. A. (2022). Onset pattern of nigrostriatal denervation in early Parkinson's disease. *Brain* 145, 1018–1028. doi: 10.1093/brain/awab378
- Prasuhn, J., Neumann, A., Strautz, R., Dreischmeier, S., Lemmer, F., Hanssen, H., et al. (2021). Clinical MR imaging in Parkinson's disease: how useful is the swallow tail sign. *Brain Behav.* 11:e02202. doi: 10.1002/brb3.2202
- Rosjat, N., Wang, B. A., Liu, L., Fink, G. R., and Daun, S. (2021). Stimulus transformation into motor action: dynamic graph analysis reveals a posterior-to-anterior shift in brain network communication of older subjects. *Hum. Brain Mapp.* 42, 1547–1563. doi: 10.1002/hbm.25313
- Shaked, D., Katzel, L. I., Seliger, S. L., Gullapalli, R. P., Davatzikos, C., Erus, G., et al. (2018). Dorsolateral prefrontal cortex volume as a mediator between socioeconomic status and executive function. *Neuropsychology* 32, 985–995. doi: 10.1037/neu0000484
- Suo, X., Lei, D., Li, N., Cheng, L., Chen, F., Wang, M., et al. (2017). Functional brain connectome and its relation to Hoehn and Yahr stage in Parkinson disease. *Radiology* 285, 904–913. doi: 10.1148/radiol.2017162929
- Tessitore, A., Esposito, F., Vitale, C., Santangelo, G., Amboni, M., Russo, A., et al. (2012). Default-mode network connectivity in cognitively unimpaired patients with Parkinson disease. *Neurology* 79, 2226–2232. doi: 10.1212/WNL.0b013e31827689d6
- Thambisetty, M., Wan, J., Carass, A., An, Y., Prince, J. L., and Resnick, S. M. (2010). Longitudinal changes in cortical thickness associated with normal aging. *NeuroImage* 52, 1215–1223. doi: 10.1016/j.neuroimage.2010.04.258
- Thomann, P. A., Wüstenberg, T., Nolte, H. M., Menzel, P. B., Wolf, R. C., Essig, M., et al. (2013). Hippocampal and entorhinal cortex volume decline in cognitively intact elderly. *Psychiatry Res.* 211, 31–36. doi: 10.1016/j.psychres.2012.06.002
- Tolosa, E., Garrido, A., Scholz, S. W., and Poewe, W. (2021). Challenges in the diagnosis of Parkinson's disease. *Lancet Neurol.* 20, 385–397. doi: 10.1016/S1474-4422(21)00030-2
- Tseriotis, V. S., Mavridis, T., Eleftheriadou, K., Konstantis, G., Chlorogiannis, D. D., Pavlidis, P., et al. (2024). Loss of the "swallow tail sign" on susceptibility-weighted imaging in the diagnosis of dementia with Lewy bodies: a systematic review and meta-analysis. *J. Neurol.* 271, 3754–3763. doi: 10.1007/s00415-024-12381-6
- van Dun, K., Brinkmann, P., Depestele, S., Verstraelen, S., and Meesen, R. (2022). Cerebellar activation during simple and complex bimanual coordination: an activation likelihood estimation (ALE) Meta-analysis. *Cerebellum* 21, 987–1013. doi: 10.1007/s12311-021-01261-8



- Vecchio, F., Miraglia, F., Alù, F., Judica, E., Cotelli, M., Pellicciari, M. C., et al. (2022). Human brain networks in physiological and pathological aging: reproducibility of electroencephalogram graph theoretical analysis in cortical connectivity. *Brain Connect.* 12, 41–51. doi: 10.1089/brain.2020.0824
- Wagner, K. H., Cameron-Smith, D., Wessner, B., and Franzke, B. (2016). Biomarkers of aging: from function to molecular biology. *Nutrients* 8:338. doi: 10.3390/nu8060338
- Wagner, M. J., Savall, J., Hernandez, O., Mel, G., Inan, H., Rumyantsev, O., et al. (2021). A neural circuit state change underlying skilled movements. *Cell* 184, 3731–3747.e21. doi: 10.1016/j.cell.2021.06.001
- Wang, Y., Hao, L., Zhang, Y., Zuo, C., and Wang, D. (2019). Entorhinal cortex volume, thickness, surface area and curvature trajectories over the adult lifespan. *Psychiatry Res. Neuroimaging* 292, 47–53. doi: 10.1016/j.psychres.2019.09.002
- Zalesky, A., Cocchi, L., Fornito, A., Murray, M. M., and Bullmore, E. (2012). Connectivity differences in brain networks. *NeuroImage* 60, 1055–1062. doi: 10.1016/j.neuroimage.2012.01.068
- Zalesky, A., Fornito, A., and Bullmore, E. T. (2010). Network-based statistic: identifying differences in brain networks. *NeuroImage* 53, 1197–1207. doi: 10.1016/j.neuroimage.2010.06.041
- Zhan, C., Chen, H. J., Gao, Y. Q., and Zou, T. X. (2019). Functional network-based statistics reveal abnormal resting-state functional connectivity in minimal hepatic encephalopathy. *Front. Neurol.* 10:33. doi: 10.3389/fneur.2019.00033
- Zhang, H., Bai, X., and Diaz, M. T. (2021). The intensity and connectivity of spontaneous brain activity in a language network relate to aging and language. *Neuropsychologia* 154:107784. doi: 10.1016/j.neuropsychologia.2021.107784
- Zhou, Y. (2021). Joint imaging applications in general neurodegenerative disease: Parkinson's, frontotemporal, Vascular Dementia and Autism. Hauppauge, NY: Nova Science Publishers.
- Zuo, C., Suo, X., Lan, H., Pan, N., Wang, S., Kemp, G. J., et al. (2023). Global alterations of whole brain structural connectome in Parkinson's disease: a Meta-analysis. *Neuropsychol. Rev.* 33, 783–802. doi: 10.1007/s11065-022-09559-y